

Open Access Article

## Distribution Pattern Identification of Mineral using XRF and XRD Method in Jeneberang Watershed, Indonesia

Muhammad Altin Massinai\*, Wahyuningsih Mamudi, Muhammad Fawzy Ismullah Massinai

Geophysics Department, Hasanuddin University, Makassar 9045, Indonesia

**Abstract:** Research has been conducted using XRF (X-Ray Fluorescence) and XRD (X-Ray Diffraction) to determine the distribution pattern and Si and Fe content and the mineral composition rocks Jeneberang Watershed. This study's main objective was to determine the metal element content and mineral composition in rock samples along the Jeneberang watershed. The minerals come from Lompobattang and Sapaya Volcano Products. The results showed that five metal elements are dominated by Si and Fe and 15 minerals found in the study area. In addition, it showed a relatively high percentage of Si, Fe, Ca, K, Al, Albite, Feldspar, and Anorthite. The Si and Fe exist in every sampling location. However, their levels are low in two locations (Bissua and Kampili), approximately 4.52% of Si and 5.79% of Fe. On the other hand, their percentage is relatively high in the rest of the sampling locations (Mawang, Sungguminasa, Malengkeri, and Barombong). Similar to the previous elements, Ca exists in every single sampling location. While the low concentration of Ca was shown in Bissua, Mawang, Sungguminasa, Malengkeri, Barombong, its concentration is very high in Kampili. Furthermore, Al and K's low concentrations were found in Bissua, Mawang, Sungguminasa, Malengkeri, and Barombong but absent in Kampili. The rapid and environment-friendly method of the modal analysis of rocks here may help map volcanic eruption flow in the Jeneberang watershed.

**Keywords:** metal element content, mineral composition, rock, X-Ray fluorescence method, X-Ray diffraction method.

## 使用 X 射线荧光和 X 射线衍射法在印度尼西亚杰内伯朗流域进行矿物分布模式识别

**摘要:** 已经使用 X 射线荧光和 X 射线衍射进行了研究, 以确定分布模式、硅和福莱姆含量以及杰内伯朗流域岩石的矿物成分。本研究的主要目的是确定杰内伯朗流域岩石样品中的金属元素含量和矿物成分。矿物质来自跳跳台和哇火山产品。结果表明, 研究区发现的 5 种金属元素以硅、福莱姆为主, 矿物有 15 种。此外, 它显示出较高百分比的硅、福莱姆、钙、钾、铝、钠长石、长石和钙长石。硅和铁存在于每个采样位置。然而, 它们在两个位置 (比苏阿和坎皮利) 的含量较低, 大约为 4.52% 的硅和 5.79% 的福莱姆。另一方面, 在其他采样地点 (马旺、松古米纳萨、马伦克里和巴隆邦), 他们的百分比相对较高。与前面的元素类似, 钙存在于每个采样位置。虽然在比苏阿、马旺、圣古米娜萨、马伦克、巴龙邦的钙浓度较低, 但在坎皮利的浓度非常高。此外, 在比苏阿、马旺、圣古米娜萨、马伦克和巴龙邦发现了低浓度的铝和钾, 但在坎皮利中不存在。此处对岩石进行模态分析的快速且环保的方法可能有助于绘制杰内伯朗流域的火山喷发流图。

**关键词:** 金属元素含量、矿物成分、岩石、X 射线荧光法、X 射线衍射法。

## 1. Introduction

Jeneberang watershed is an area that is flowed by a

Received: March 10, 2021 / Revised: April 11, 2021 / Accepted: May 13, 2021 / Published: June 28, 2021

About the authors: Muhammad Altin Massinai, Wahyuningsih Mamudi, Muhammad Fawzy Ismullah Massinai, Geophysics Department, Hasanuddin University, Makassar, Indonesia

Corresponding author Muhammad Altin Massinai, [altin@science.unhas.ac.id](mailto:altin@science.unhas.ac.id)

river from Lompobattang Mount to the Makassar Strait. This river is a volcanic eruption flow of Lompobattang. This eruption leads to releasing materials magma from the earth, carrying rocks and ash gushed Jeneberang and surrounding watersheds [1].

In general, the forming process of mineral deposits in the Jeneberang watershed, both metal, and nonmetal, can be formed due to mineralization caused by the volcanic activity of Lompobattang [2]. However, the minerals that make up the magma are not formed simultaneously or in the same conditions [3]. Certain minerals will be crystallized at higher temperatures than other minerals [4]. The formation of various minerals in nature will produce various types of rock, which is structured into the material's chemical composition and physical properties. Therefore, to

obtain information about the content of metal elements, especially Si and Fe and the percentage composition of minerals in rocks, as well as the spread pattern of distribution along the Jeneberang watershed downstream, this research was conducted using XRF (X-Ray Fluorescence) and XRD (X-Ray Diffraction) method [5], [6], [7], [8], [9], [10], [11].

Si is found in nature in the form of the mineral quartz. Most of the earth's crust consists of silicate rocks [12]. Si is used in the ceramic industry, glass, and paper. Silica is generally heat resistant and abrasives in the industry—derivation of Si-shaped olivine, quartz, feldspar, and mica. Fe is widely used as nickel steel, armament equipment, steel, and household appliances [13], [14], [15].

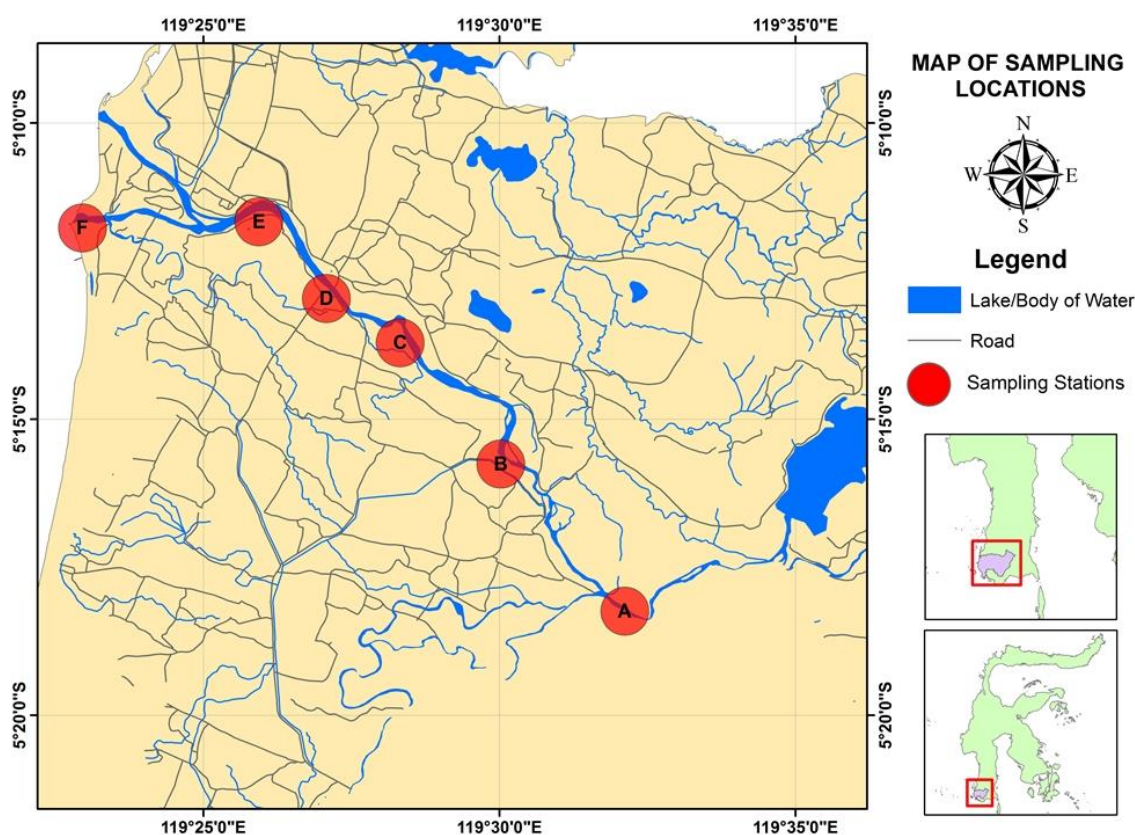


Fig. 1 Study area map of Jeneberang watershed in South Sulawesi, Indonesia (modified from [16])

This research was conducted by taking test samples at the Jeneberang watershed (Fig. 1). The samples were analyzed to know the concentration of Si and Fe and their mineral composition in the laboratory using XRF and XRD methods. The rapid and environment-friendly method of the modal analysis of rocks here may be useful for mapping volcanic eruption flow in the Jeneberang watershed.

## 2. Research Methodology

This research was conducted by taking rock samples at several points in the Jeneberang river flow of Gowa Regency, which will then be examined and analyzed in the laboratory. The location of the rock sampling point

is astronomically located at coordinates  $119^{\circ} 16'15.83''E - 120^{\circ} 45'4.25''E$  and  $05^{\circ} 5'47.99''LS - 05^{\circ} 23'1.68''LS$ . Geographically, the research location, which is the Jeneberang river flow, includes cities including Bilibili, Sungguminasa, and Makassar. The sampling locations are as follows: Bissua (A), Kampili (B), Mawang (C), Sungguminasa (D), Malengkeri (E), and Barombong (D).

The data used in this study are primary. The sampling process is done directly at several points along the Jeneberang watershed [17]. Field survey and location determination were done using the Geological Map Sheet of Ujungpandang and GPS [18]. The distribution of sample points refers to the geological

map representing the state of the samples taken in the field.

Laboratory analysis is an important stage for knowing rocks' physical and chemical properties that cannot be done directly in the field. This analysis uses a variety of current methods and tools. For example, the laboratories use XRF and XRD to produce the rocks' minerals types [19], [20]. In addition, the composition and the percentage of mineral elements were used in the generation of mineral distribution patterns.

At this stage, the results of the chemical composition and mineral composition of the content test using XRF (X-Ray Fluorescence) and XRD (X-Ray Diffraction) were analyzed using the Match program to produce the composition and percentage of mineral content. This data will support each other and determine data validation. Furthermore, the composition and percentage of elemental content will be used in making the distribution patterns of elements that dominate the content of these rocks.

### 3. Results

The results of each rock sample's content in the laboratory using XRF and XRD instruments can be seen in Table 1. The form of the content of each rock sample in the laboratory using the XRF and XRD instrument can be seen in Table 1. The form of the chemical composition refers to the geological condition of the study area.

Table 1 Test results of chemical composition measurement

The percentage of results measurements using XRF						
No	Samples	Element name				
		Si	Fe	Ca	K	Al
1	A	52.16	14.24	11.13	11.04	7.83
2	B	4.52	5.79	83.63	-	-
3	C	46.02	22.02	18.26	2.95	7.37
4	D	44.03	30.43	3.60	5.75	10.59
5	E	41.62	31.32	7.83	4.97	8.17
6	F	44.97	25.82	11.60	5.63	6.01

The result of mineral composition measurement with analysis software match can be seen in Table 2.

Table 2 Mineral composition analysis

No	Samples	Minerals	%
1	A	Albite	54.9
		Feldspar	40.8
		Sanidine	4.2
2	B	Magnesiocapholite	34.2

		Panitite	22.9
		Potassium Magnesium Silicate	21.1
		Pentahydrate	18.7
		Strontiumtellurite	3.1
		Calcium tecto-dialumodisilicate	64.7
		Anorthite	
3	C	Potassium Magnesium Silicate	18.0
		Feldspar	14.8
		Barium Ferro Stibium Sulfide	2.4
		Anorthite	77.0
		Mereiterite	13.0
		Potassium manganese (II) polyvanadate	10.0
4	D	Enstatite	36.5
		Anorthite	27.3
		Albite	23.9
		Anorthoclase	12.3
		Orthoclase	48.4
		Feldspar	24.4
5	E	Iron (III) fluoride hydrate (third / .33)	21.5
		Potassium-alumotrisilicatetecto	5.7
		Sanidine	

Table 2 shows the contained minerals in rock samples that were observed in the form of Albite, Feldspar, Sanidine, Magnesiocapholite, Panitite, Pentahydrate, Strontium Tellurite, Calcium Tectodialumodisilicate Anorthite, Anorthite, Mereiterite, Potassium Manganese (II) Polyvanadate, Enstatite, Anorthoclase, Iron (III) Fluoride Hydrate (1/3 /.33), Potassium Tectoalumotrisilicate Sanidine.

### 4. Discussion

In this study, there were six sampling sites, including three samples in the form of rocks, two samples of sand form, and one sample of the clay form. That is due to the condition of research sites located on the flow of the Jeneberangriver. Below is the composition of elements and mineral contained in each sample:

Sample A is a form of rocks in shape. The rock found in the area was a Sapaya volcanic (lava, breccias, tuffs, and conglomerates) [17]. Rock samples taken from the field were identified as acid igneous rocks because of the content of SiO<sub>2</sub> (68.31%) [2]. XRF results to the rock's chemical composition were dominated by 52.16% of Si, 14% of Fe, 11.13% of Ca, 11.04% of K, 7.83% of Al, and 3.6% of other elements. Based on the test results using XRD tools, these rocks

contain 54.9% of Albite, 40.8% of feldspar, and 4.2% of Sanidine.

These minerals are products of the Late Miocene eruption of Sapaya volcano and Lompobattang volcanic products, Pleistocene age. Location sample A (Bissua) is the meeting point of the Lompobattang volcanic lava flow (Qlv) with the Sapaya volcanic lava flow (Tpsv).

Sample B is a form of rock in shape. In this location, it was noticed that there are alluvial deposits (gravel, sand, clay, silt, and limestone coral). Based on examining rock samples taken from the field, these rocks were identified as sedimentary rocks. Contact between limestone coral with breccias can be observed on the chunk of the sample. In addition, cloudy white to brown Limestone was composed of marine organisms. That may indicate that the area is an ex-marine area that was uplifted and precipitated, which caused the contact [3].

From the XRF (X-Ray fluorescence) analysis to the chemical composition, the rock is dominated by Ca (83.63%) and completed by Fe 5.79%, Si. Based on the results of the test mineral content using an XRD, these rocks contain minerals Magnesiochalcophyllite (34.2%), Panitite (22.9%), Potassium Magnesium Silicate (21.1%), Pentahydrate 18.7%, and Strontium Tellurite (3.1%).

Seeing the minerals found in sample location B (Kampili) consist of minerals originating from igneous rocks from the Sapaya volcanic products, which have experienced weathering [16]. The sediment from this weathering process is associated with deep-sea corals in the Late Miocene. Then it was raptured at the beginning of the Pleistocene. At this time, lowlands were formed in Kampili.

Sample C (Mawang) is a form of rock in shape. Samples were identified as igneous rocks. The river's alluvial deposits, the beach (gravel, sand, clay, silt, and limestone coral) are in the sample locations [2]. The measurement results of XRF to the chemical composition of the rock are dominated by elements of the Si (46.02%), Fe (22.02%), Ca (18.26%), Al (7.37%), K (2.95%), and other elements up to 3.8%. On the other hand, the test results using the tool XRD mineral content showed that these rocks contain minerals Calcium-Dialumodisilicate Tecto Anorthite (64.7%), Potassium Magnesium Silicate (18.0%), Feldspar (14.8%), and Barium Ferro Stibium Sulfide (2.4%).

The difference between the interpretation of the geological map and the results of this study makes it imperative to edit this area's geological map in an up-to-date and accurate manner. This area is the area of the Sapaya volcano lava flow.

Sample D (Sungguminasa) was found in clay on the edge of the Jeneberang river flow. The area is dominantly influenced by river and coastal alluvium

(gravel, sand, clay, silt, and limestone coral) [2]. The measurement results of XRF to the chemical composition of the alluvial deposits of the river is dominated by the element of Si (44.03%), Fe (30.43%), Al (10.59%), K (5.75%), Ca (3.60%), and other elements up to 5.6%. Furthermore, the results of the test mineral content using XRD tool mud sediment contain mineral Anorthite (77.0%), Mereiterite (13.0%), and Potassium Manganese (II) polyvanadate (10.0%).

This area is a lowland area that is affected by a flood area. The minerals in this area are the location for deposition through the Jeneberang river. Therefore, these minerals are minerals sent from the upper reaches of the Jeneberang river, is the ancient Lompobattang volcano.

Sample E (Malengkeri) is a form of sand in shape. Samples in this region consist of alluvial deposits of the river and the coast in gravel, sand, clay, silt, and limestone coral [2]. The XRF measurement results of the sediment content are dominated by the five elements, namely the Si (41.62%), Fe (31.32%), Al (8.17%), Ca (7.83%), K (4.97%), and the combined elements up to 6.09%. Moreover, the results of mineralogical testing using the XRD tool showed its content in the form of Enstatite (36.5%), Anorthite (27.3%), Albite (23.9%), and Anorthoclase (12.3%). Thus, this sample was weathering the basalt rock from the Sapaya volcanic products associated with the Makassar Strait coast's sand deposits.

Sample F (Barombong) in the form of sand is located in the Barombong area. The site's geological conditions consist of the alluvial deposits of the river and the coast in gravel, sand, clay, silt, and limestone coral. XRF instrument readings the sediment content is dominated by the five elements, namely the Si (44.97%), Fe (25.82%), Ca (11.60%), Al (6.01%), K (5.63%), and combined elements up to 5.97%. On the other hand, the results of mineralogical testing using the XRD tool shows its content in the form of Orthoclase (48.4%), Feldspar (24.4%), Iron (III) Fluoride Hydrate (1/3/.33), 21.5%, and Potassium Tecto-Alumotrisilicate sanidine (5.7%).

This sample's location is in the downstream area, in the city of Makassar, South Sulawesi. Minerals in the Barombong area are products of the Sapaya Volcano and Lompobattang Volcano. Sapaya volcano is Late Miocene, while Lompobattang volcano is Pleistocene. The rocks from the two volcanoes are weathered and deposited through the Jeneberang river to the Barombong beach.

The areas of Malengkeri, Sungguminasa, and Barombong are downstream. Therefore Si and Fe elements from the three regions are relatively high compared to other regions. The Mawang area has a high Si value because around this area, and karst hills contain Limestone. Mineral  $\text{SiO}_2$  is a constituent of Limestone, so this area is rich in Si.

Silicon and Ferrum in this area are due to the sediment from the eruption of volcanoes. There are two volcanoes in this area. They are Lompobattang and Sapaya, which are Pleistocene and Neogen in age, respectively. Both volcanoes are upstream of rivers in the Jeneberang watershed.

In this area, the minerals are volcanic products associated with coral reefs from the deep sea. It is a phenomenon that needs attention in tropical regions that have volcanoes and deep seas. Coral reefs are very fertile in the tropics.

## 5. Conclusions

From the research that has been done, it can be concluded that:

1. Minerals formed in the research area are volcanic products associated with coral reefs from the deep sea.
2. Metal and mineral elements are the products of the ancient volcanoes of Sapaya and the ancient volcanoes of Lompobattang.
3. Metals and a mineral composition contained in the rocks along the river are Jeneberang are as follows:
  - a. Metal elements: Si, Fe, Ca, K, and Al
  - b. Minerals: Feldspar, Albite, Anorthite, Sanidine, Magnesiochapholite, Panitite, Pentahydrate, Mereiterite, Potassium Manganese (II) Polyvanadate, Enstatite, Anorthoclase, Orthoclase, Iron (III) Fluoride Hydrate (1/3/.33), Potassium Tectoalumotrisilicate Sanidine.
4. The distribution pattern of metal elements:
  - a. Si and Fe exist in every sampling location. Their levels are relatively high in Mawang, Sungguminasa, Malengkeri, and Barombong, even though those are low in Kampili.
  - b. Ca levels are low in Bissua, Mawang, Sungguminasa, Malengkeri, Barombong but very high in Kampili
  - c. Al is found in Bissua, Mawang, Sungguminasa, Malengkeri, Barombong at a low levels, whereas this element is absent in Kampili.
  - d. K levels are very low in Bissua, Mawang, Sungguminasa, Malengkeri, Barombong whereas this element is absent in Kampili.
  - e. Si and Fe correlate with the depositional environment.

## References

[1] MASSINAI M. A., SUDRADJAT A., and LANTU. The Influence of Seismic Activity in South Sulawesi Area to the Geomorphology of Jeneberang Watershed. *International Journal of Engineering and Technology*, 2013, 10: 945–948. <https://core.ac.uk/download/pdf/25493429.pdf>

[2] YUWONO Y. S. Mineralogy and Petrology of Lompobattang Stratovolcano, South Sulawesi (in Indonesian). *Geology Indonesia*, 1989, 12: 489–509.

[3] POLVE M., MAURY R. C., BELLON H., RANGING

C., PRIADI B., YUWONO Y. S., JORON J. L., and SOERIA-ATMADJA R. Magmatic Evolution of Sulawesi (Indonesia): Constrains on the Cenozoic Geodynamic History of the Sundaland Active Margin. *Tectonophysics*, 1997, 272: 69–92. [https://doi.org/10.1016/S0040-1951\(96\)00276-4](https://doi.org/10.1016/S0040-1951(96)00276-4)

[4] WANG X., LI J., ZHANG N., XIE J., LIANG D., and DENG L. Evolution of Hyperfine Structure and Magnetic Characteristic in Fe-Si-Cr Alloy with Increasing Heat Treatment Temperature. *Materials and Design*, 2016, 96: 314–322. <https://doi.org/10.1016/j.matdes.2016.02.031>

[5] BOUCHARD M., & JOLICOEUR S. Chemical Weathering Studies in Relation to Geomorphological Research in Southeastern Canada. *Geomorphology*, 2000, 32: 213–238. [https://doi.org/10.1016/S0169-555X\(99\)00098-7](https://doi.org/10.1016/S0169-555X(99)00098-7)

[6] O'CONNOR F., CHEUNG W. H., and VALIX M. Reduction Roasting of Limonite Ores: Effect of Dehydroxylation. *International Journal of Mineral Processing*, 2016, 80: 88–99. <https://doi.org/10.1016/j.minpro.2004.05.003>

[7] PELTONEN P., KONTINEN A., HUHMA H., and KURONEN U. Outokumpu Revisited: New Mineral Deposit Model for the Mantle Peridotite-Associated Cu–Co–Zn–Ni–Ag–Au Sulphide Deposits. *Ore Geology Reviews*, 2008, 33: 559–617. <https://doi.org/10.1016/j.oregeorev.2007.07.002>

[8] AIGLSPERGER T., PROENZA J. A., LEWIS J. F., LABRADOR M., SVOJTKA M., ROJAS-PURÓN A., LONGO F., and ĐURIŠOVÁ J. Critical Metals (REE, Sc, PGE) in Ni Laterites from Cuba and the Dominican Republic. *Ore Geology Reviews*, 2016, 73: 127–147. <https://doi.org/10.1016/j.oregeorev.2015.10.010>

[9] CHEN D., XIAO J., and ZHAN J. Preparation and Characterization on  $Mn_xMg_{1-x}Fe_2O_4$  Nanoparticles by Ultrasonic-Assisted Ball Milling. *Journal of Hunan University: Natural Sciences*, 2018, 45(6): 51–55. <https://doi.org/10.16339/j.cnki.hdxzbzkb.2018.06.008>

[10] SONG Y., WANG Z., LIU Y., QU Q., and YANG M. Research on Stress Corrosion Behavior of AZ91 Magnesium Alloy Modified by Erbium and Cerium. *Journal of Hunan University: Natural Sciences*, 2018, 45(6): 22–27. <https://doi.org/10.16339/j.cnki.hdxzbzkb.2018.06.003>

[11] YAN H., ZENG Y., and CHEN X. Study on Preparation and Mechanical Properties of Graphene/Polyurethane Nanocomposites. *Journal of Hunan University: Natural Sciences*, 2018, 45(6): 45–50. <https://doi.org/10.16339/j.cnki.hdxzbzkb.2018.06.007>

[12] GAO P., ZHAO Z. F., and ZHENG Y. F. Magma Mixing in Granite Petrogenesis: Insights from Biotite Inclusions in Quartz and Feldspar of Mesozoic Granites from South China. *Journal of Asian Earth Sciences*, 2016, 123: 142–161. <https://doi.org/10.1016/j.jseae.2016.04.003>

[13] LAZNICKA P. Giant Metallic Deposits — A Century of Progress. *Ore Geology Reviews*, 2014, 62: 259–314. <https://doi.org/10.1016/j.oregeorev.2014.03.002>

[14] LUO J., LI G., RAO M., PENG Z., ZHANG Y., and JIANG T. Atmospheric Leaching Characteristics of Nickel and Iron in Limonitic Laterite with Sulfuric Acid in the Presence of Sodium Sulfite. *Minerals Engineering*, 2015, 78: 38–44. <https://doi.org/10.1016/j.mineng.2015.03.030>

[15] ZHAO Q., QIAN Z., CUI X., WU Y., and LIU X. Influences of Fe, Si and Homogenization on Electrical Conductivity and Mechanical Properties of Dilute Al-Mg-Si alloy. *Journal of Alloys and Compounds*, 2016, 666: 50–57.

<https://doi.org/10.1016/j.jallcom.2016.01.110>

[16] MASSINAI M. A., KADIR F. H., MASSINAI M. F. I., and ASWAD S. Morphostructure Analysis of Sapaya Ancient Volcanic Area Based Lineament Data. *American Institute of Physics Conference Proceedings*, 2015, 1730(1). <https://doi.org/10.1063/1.4947399>

[17] MASSINAI M. A., SYAMSUDDIN E., PAHARUDDIN, MASSINAI M. F. I., and MADDA M. A. Mapping Groundwater Potential Based on Geospatial Analysis and Multi-Criteria Decision Analysis in Gowa Regency, South Sulawesi, Indonesia. *Journal of Advanced Research in Dynamical and Control Systems*, 2020, 12(5): 550–561. <http://doi.org/10.5373/JARDCS/V12I5/20201974>

[18] DARMAN H., & SIDI H. *An Outline of The Geology of Indonesia*. Indonesian Association of Geologists, Jakarta, Indonesia, 2000. <https://www.worldcat.org/title/outline-of-the-geology-of-indonesia/oclc/48203047>

[19] PICKLES C. A. Microwave Heating Behavior of Nickeliferous Limonitic Laterite Ores. *Minerals Engineering*, 2004, 17: 775–784. <https://doi.org/10.1016/j.mineng.2004.01.007>

[20] ELIOPOULOS D. G., ECONOMOU-ELIOPOULOS M., APOSTOLIKAS A., and GOLIGHTLY J. P. Geochemical Features of Nickel-Laterite Deposits from the Balkan Peninsula and Gordes, Turkey: The Genetic and Environmental Significance of Arsenic. *Ore Geology Reviews*, 2012, 48: 413–427. <https://doi.org/10.1016/j.oregeorev.2012.05.008>

#### 参考文献:

[1] MASSINAI M. A., SUDRADJAT A., 和 LANTU. 南苏拉威西地区地震活动对杰内伯朗流域地貌的影响. *国际工程技术杂志*, 2013, 10: 945–948. <https://core.ac.uk/download/pdf/25493429.pdf>

[2] YUWONO Y. S. 南苏拉威西岛隆波巴当成层火山的矿物学和岩石学 (印度尼西亚语). *地质印度尼西亚*, 1989, 12: 489–509.

[3] POLVE M., MAURY R. C., BELLON H., RANGING C., PRIADI B., YUWONO Y. S., JORON J. L., 和 SOERIA-ATMADJA R. 苏拉威西岛 (印度尼西亚) 的岩浆演化: 对巽他大陆活动边缘新生代地球动力学历史的制约. *构造物理学*, 1997, 272: 69–92. [https://doi.org/10.1016/S0040-1951\(96\)00276-4](https://doi.org/10.1016/S0040-1951(96)00276-4)

[4] WANG X., LI J., ZHANG N., XIE J., LIANG D., 和 DENG L. 铁硅铬合金随着热处理温度的升高超精细组织和磁特性的演变. *材料和设计*, 2016, 96: 314–322. <https://doi.org/10.1016/j.matdes.2016.02.031>

[5] BOUCHARD M., 和 JOLICOEUR S. 与加拿大东南部地貌研究相关的化学风化研究. *地貌学*, 2000, 32: 213–238. [https://doi.org/10.1016/S0169-555X\(99\)00098-7](https://doi.org/10.1016/S0169-555X(99)00098-7)

[6] O'CONNOR F., CHEUNG W. H., 和 VALIX M. 褐铁矿的还原焙烧: 脱羟基的影响. *国际矿物加工杂志*, 2016, 80: 88–99. <https://doi.org/10.1016/j.minpro.2004.05.003>

[7] PELTONEN P., KONTINEN A., HUHMA H., 和 KURONEN U. 重新审视奥托昆普: 地幔橄榄岩伴生银金镍钴铜锌硫化物矿床的新矿床模型. *矿石地质评论*, 2008, 33: 559–617. <https://doi.org/10.1016/j.oregeorev.2007.07.002>

[8] AIGLSPERGER T., PROENZA J. A., LEWIS J. F., LABRADOR M., SVOJTKA M., ROJAS-PURÓN A., LONGO F., 和 ĀURIŠOVÁ J. 古巴和多米尼加共和国镍红土中的关键金属 (稀土元素、钷、铂族元素). *矿石地质评论*, 2016, 73: 127–147. <https://doi.org/10.1016/j.oregeorev.2015.10.010>

[9] CHEN D., XIAO J., 和 ZHAN J. 超声波辅助球磨法制备锰镁 1x-x 铁 2 氧 4 纳米颗粒及其表征. *湖南大学学报: 自然科学*, 2018, 45(6): 51–55. <https://doi.org/10.16339/j.cnki.hdxzbzkb.2018.06.008>

[10] SONG Y., WANG Z., LIU Y., QU Q., 和 YANG M. 钕钪改性铝锌 91 镁合金应力腐蚀行为研究. *湖南大学学报: 自然科学*, 2018, 45(6): 22–27. <https://doi.org/10.16339/j.cnki.hdxzbzkb.2018.06.003>

[11] YAN H., ZENG Y., 和 CHEN X. 石墨烯/聚氨酯纳米复合材料的制备及力学性能研究. *湖南大学学报: 自然科学*, 2018, 45(6): 45–50. <https://doi.org/10.16339/j.cnki.hdxzbzkb.2018.06.007>

[12] GAO P., ZHAO Z. F., 和 ZHENG Y. F. 花岗岩成因中的岩浆混合: 华南中生代花岗岩石英和长石中黑云母包裹体的洞察. *亚洲地球科学杂志*, 2016, 123: 142–161. <https://doi.org/10.1016/j.jseaes.2016.04.003>

[13] LAZNICKA P. 巨大的金属矿床——一个世纪的进步. *矿石地质评论*, 2014, 62: 259–314. <https://doi.org/10.1016/j.oregeorev.2014.03.002>

[14] LUO J., LI G., RAO M., PENG Z., ZHANG Y., 和 JIANG T. 亚硫酸钠存在下硫酸对褐铁矿红土中镍和铁的大气浸出特性 [J]. *矿产工程*, 2015, 78: 38–44. <https://doi.org/10.1016/j.mineng.2015.03.030>

[15] ZHAO Q., QIAN Z., CUI X., WU Y., 和 LIU X. 铁、硅和均质化对稀铝镁硅合金电导率和机械性能的影响. *合金与化合物杂志*, 2016, 666: 50–57. <https://doi.org/10.1016/j.jallcom.2016.01.110>

[16] MASSINAI M. A., KADIR F. H., MASSINAI M. F. I., 和 ASWAD S. 基于线材数据的沙巴古火山区形态结构分析. *美国物理学会会议论文集*, 2015, 1730(1). <https://doi.org/10.1063/1.4947399>

[17] MASSINAI M. A., SYAMSUDDIN E., PAHARUDDIN, MASSINAI M. F. I., 和 MADDA M. A. 印度尼西亚南苏拉威西戈瓦摄政 基于地理空间分析和多标准决策分析的地下水潜力绘图. *动力与控制系统高级研究杂志*, 2020, 12(5): 550–561.

<http://doi.org/10.5373/JARDCS/V12I5/20201974>

[18] DARMAN H., & SIDI H. 印度尼西亚地质概况。印度尼西亚地质学家协会，印度尼西亚雅加达，2000.

<https://www.worldcat.org/title/outline-of-the-geology-of-indonesia/oclc/48203047>

[19] PICKLES C. A. 含镍褐铁矿红土矿石的微波加热行为。矿产工程，2004，17：775-784.

<https://doi.org/10.1016/j.mineng.2004.01.007>

[20] ELIOPOULOS D. G., ECONOMOU-ELIOPOULOS M., APOSTOLIKAS A., 和 GOLIGHTLY J. P. 土耳其巴尔干半岛和戈尔德镍红土矿床的地球化学特征：砷的遗传和环境意义。矿石地质评论，2012，48：413-427.

<https://doi.org/10.1016/j.oregeorev.2012.05.008>